

Ageing-Aware Deep Reinforcement Learning for Adaptive Fast Charging of Li-ion Battery Considering Coupled Degradation mechanisms

Ben Shang ^{1,2}, Yinglong He ^{1*}, Lei Wang ^{3*}, Zeyu Sun ⁴, Jianwei Shao ⁵, Constantina Lekakou ¹, Jing Zhao ⁶, Youping Fan ^{2*}

1 School of Mechanical Engineering Sciences, University of Surrey, Guildford, UK

2 Institute of Next Generation Power Systems and International Standards, Wuhan University, Wuhan, China

3 Institute of Nuclear and New Energy Technology, Tsinghua University, Beijing, China

4 Department of Engineering Science, University of Oxford, Oxford, UK

5 School of Electrical Engineering and Automation, Wuhan University, Wuhan, China

6 Department of Traffic Engineering, University of Shanghai for Science and Technology, Shanghai, China

(Corresponding Author: yinglong.he@surrey.ac.uk, lwang9305@tsinghua.edu.cn, ypfan@whu.edu.cn)

ABSTRACT

A major challenge in fast charging is to reduce the charging time without accelerating battery aging. The interaction between different aging mechanisms has not been investigated in the fast-charging optimization. To address this issue, we propose an adaptive, aging-aware fast charging method utilizing deep reinforcement learning to balance charging speed with the aging effects of multiple degradation mechanisms. This method incorporates a coupled degradation model to capture the dynamic characteristics of batteries throughout their lifecycle. Using deterministic policy gradient and Markov decision process (MDP) frameworks, the algorithm optimally adjusts charging currents based on safety constraints and internal coupled aging. We demonstrate the effectiveness of our approach through simulations using the PyBAMM model. Results indicate significant adaptability to variations in battery characteristics at different aging stages.

Keywords: Optimal charging control, Coupled battery model, deep reinforcement learning

NONMENCLATURE

Abbreviations

MDP	Markov Decision Process
CC-CV	Constant Current Constant Voltage
SOH	State of Health
SOC	State of Charge
DFN	Doyle-Fuller-Newman
SPM	Single Particle Model
ROM	Reduced-Order Model
DRL	Deep Reinforcement Learning
SEI	Solid Electrolyte Interphase
LAM	Loss of Active Material

LLI	Loss of Lithium Inventory (LLI)
<i>Symbols</i>	
I	Current
U	Voltage
T	Temperature

1. INTRODUCTION

The fast charging technology for lithium-ion batteries has been an active area of ongoing research. However, due to the inherent chemical characteristics of batteries, fast charging achieved by large currents can significantly accelerate battery degradation and even cause safety incidents. Therefore, designing an optimal charging strategy that minimizes charging time while maintaining battery performance and safety has received increasing attention.

Currently, fast charging strategies can be divided into passive fast-charging strategies (memory-less charging) and adaptive fast-charging strategies (memory-based charging). Passive charging strategies, such as CC-CV (Constant Current Constant Voltage), use predefined and fixed parameters that do not account for changing internal behaviors or the state of health (SOH) of the battery [1][2]. As a result, when the battery's inherent state supports higher current rates, it loses the opportunity to charge at these rates. Conversely, when lower thresholds are required due to internal dynamics, the battery might be forced to endure fixed parameters, leading to unnecessary stress. Adaptive charging strategies aim to obtain the internal state information of the battery by establishing effective battery models during the charging process, thereby controlling the charging process to protect the battery from unnecessary degradation. With advancements in battery modeling theories and machine learning technologies,

adaptive charging strategies are increasingly seen as the future direction for rapid charging technology.

Adaptive charging strategies utilize battery models that can be categorized into three main types: electrochemical models, equivalent circuit models, and data-driven models[3][4]. Equivalent circuit models can simulate the internal resistance characteristics and thermal properties of batteries without considering the chemical processes, offering fast computation speeds. For instance, Jin et al. [5] developed a fast charging strategy aimed at maximizing charging efficiency based on an enhanced equivalent circuit model (ECM) that incorporates thermal characteristics. The results demonstrated that this strategy could meet safety constraints during the battery charging process. However, these models tend to overlook the non-linear characteristics of batteries and exhibit significant errors in the low state of charge (SOC) region. Common electrochemical models include the Doyle-Fuller-Newman (DFN) model, single particle model (SPM), and reduced-order models (ROM). The advantage of these models lies in their ability to simulate the internal reaction mechanisms of batteries, but they require extensive experimentation to determine model parameters, making the modeling process costly. For example, Wu et al. [6] proposed a tri-objective optimization charging method based on an electrochemical-thermal coupled model to optimize battery charging time, energy loss, and internal temperature rise. Data-driven models employ machine learning algorithms to construct surrogate battery models. These models have low modeling costs but their accuracy depends on the quality of the training data, and the model results can be difficult to interpret. For instance, a model based on Gaussian process regression was proposed to optimize charging efficiency by Hao et al. [7], capable of calculating external characteristics such as temperature, SOC, and voltage during the charging process under various aging conditions.

It has been shown that there are still several shortcomings despite the valuable explorations in adaptive fast charging optimization in the literature:

(1) Modeling Aspect: most of the aforementioned work has been focused on individual degradation mechanisms. The interaction between more than two degradation mechanisms has not been investigated in the control algorithm development.

(2) Optimization Objective Design: The mentioned studies primarily aim to maximize charging efficiency under voltage and temperature safety constraints. Few models can simulate the internal reactions of the battery

during the charging process and adjust the charging current to extend battery life.

(3) Control Strategy Design: Existing studies focus on current variations during a single charging cycle, neglecting the impact of battery aging on charging strategies over the entire life cycle.

In light of the discussion above, this paper develops an electrochemical-thermal-aging coupled battery model that considers various internal aging degradation mechanisms and their interactions, and combine it with the deep reinforcement learning algorithm to manipulate the optimal charging current considering the constraints of safe requirements and the internal coupled aging across the entire life cycle. The main contributions of this paper are as follows:

(1) An accurate DFN-based electrochemical-thermal-aging coupled model is established by analyzing the internal aging mechanisms and coupling effects of lithium plating, plated lithium-induced reactions, SEI growth, and other side reactions.

(2) By embedding the coupled aging model in the deep reinforcement learning (DRL) framework, an optimal charging strategy that accounts for changes in coupled aging characteristics over the entire lifecycle based on Mars charging theory is proposed.

(3) The simulation results based on PyBAMM show that the optimal charging strategies are strongly affected by the battery aging status and has significant adaptability to variations in battery characteristics at different aging stages.

The remainder of this paper is organized as follows: Section 2 analyzes the internal aging mechanisms and coupling effects of the battery, and introduce the development and validation of the model. Section 3 describes the proposed method, including the selection of charging currents, the design of the battery charging strategy, and the training of the deep learning model. Section 4 discusses and compares the simulation results on the PyBAMM model. Finally, conclusions are given in Section 5.

2. BATTERY ELECTROCHEMICAL COUPLED MODEL

2.1 Degradation mechanisms and interactions

Four primary degradation mechanisms occur in Li-ion batteries: (1) SEI layer growth, (2) particle cracking, (3) loss of active material, and (4) lithium plating [1]. Generally, the battery exhibits a nonlinear aging characteristic, which can be divided into three stages, as illustrated in Fig. 1. The degradation phenomena and internal aging mechanisms vary significantly at different

stages. In the early-aged stage, SEI formation on the anode causes LLI, resulting in a rapid decrease in battery capacity during the initial cycles. In the moderately-aged stage, battery performance steadily declines due to various side reactions within the battery. In the fully-aged stage, there is a sharp capacity drop near the end of life, caused by rapid lithium ion inventory loss due to lithium plating, and/or active material loss due to electrolyte depletion, binder failure, and volume changes.

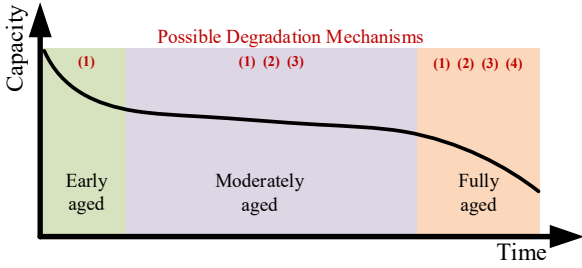


Fig. 1 Possible internal mechanism in different status

The interactions between degradation mechanisms in the negative electrode are illustrated in Fig. 2. SEI formation leads to LLI by immobilizing lithium ions and causing impedance changes through film resistance and pore clogging. Lithium plating results in LLI by forming dead lithium and contributes to impedance changes through pore clogging. Particle fracture can impact all modes of degradation: it causes LLI by enabling additional SEI formation on cracks and affects impedance changes. Additionally, these aging mechanisms influence each other. LLI generates negative feedback, as reduced cyclable lithium inhibits lithium plating by preventing the negative electrode from reaching the highly lithigated state where plating occurs. LAM triggers a positive feedback loop by enhancing particle fracture; LAM decreases the interface area between the active material and electrolyte, increasing interfacial current density and mechanical stress.

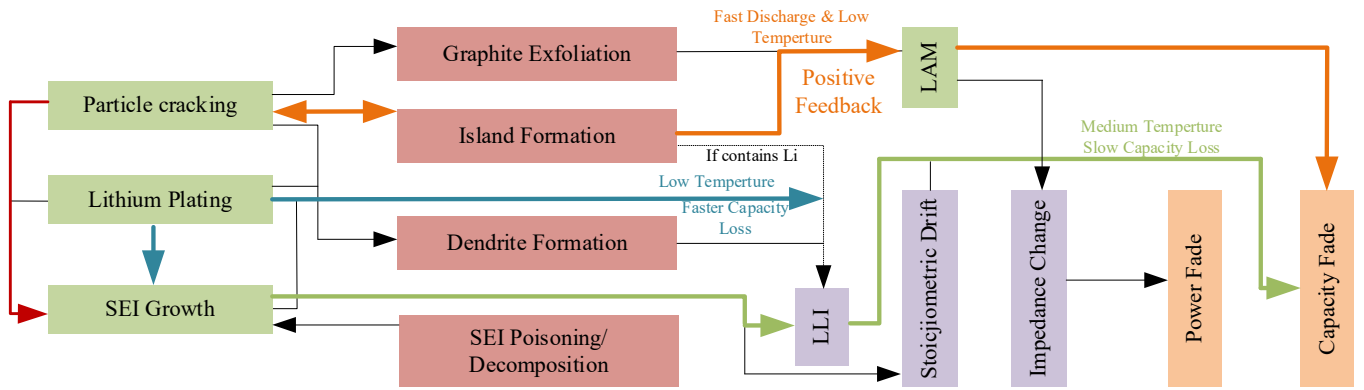


Fig.2 the interactions between degradation mechanisms in NE (Adapted from Simon et al [8])

2.2 Battery models and Governing equations

The Doyle–Fuller–Newman (DFN) model is chosen for representing the behavior of LiBs. The key equations are included here as they are useful for understanding the interaction between different degradation mechanisms. Please refer to [5] [8] for more details.

(1) SEI layer growth model

A simplified version based on solvent diffusion limited SEI growth model is used in this work. The diffusion of solvent molecules through the SEI layer limits its growth.

The thickness growth rate of the SEI layer is

$$\frac{\partial L_{SEI}}{\partial t} = -\frac{1}{2} N_{sol} \bar{V}_{SEI} = \frac{c_{slo,0} D_{sol}(T) \bar{V}_{SEI}}{2L_{SEI}} \quad (1)$$

The SEI layer is assumed to have an Ohmic

resistivity ρ_{SEI} , causing a voltage drop η_{SEI} :

$$\eta_{SEI} = \rho_{SEI} L_{SEI} \frac{j_{tot}}{a} \quad (2)$$

where j_{tot} is the interfacial current density

(2) Particle cracking model

The crack model in this work is based on the fatigue crack model in Deshpande et al. The fatigue crack growth model follows Paris' law:

$$\frac{dl_{cr}}{dN} = \frac{k_{cr}}{t_0} (\sigma_t b_{cr} \sqrt{\pi l_{cr}})^{m_{cr}} \sigma_t > 0, \quad (3)$$

where t_0 is the time for one cycle, b_{cr} is the stress intensity factor correction, k_{cr} and m_{cr} are constants that are determined from experimental data.

For interactions between the SEI growth and particle cracking, we apply the same SEI growth model on the cracks but define a very thin initial SEI layer to

consider the difference between the crack surfaces and normal surface. The averaged thickness of the SEI layer on cracks $L_{SEI,Cr}$ is:

$$\frac{\partial L_{SEI,Cr}}{\partial t} = \frac{c_{sol,0} D_{sol}(T) \bar{V}_{SEI}}{2L_{SEI,Cr}} + \frac{\partial l_{cr}}{\partial t} \frac{L_{SEI,Cr0} - L_{SEE,Cr}}{l_{cr}} \quad (4)$$

(3) loss of active material model

Only LAM as a consequence of particle cracking is included here. The decrease in the accessible volume fraction of active materials ϵ_a is estimated by

$$\frac{\partial \epsilon_a}{\partial t} = \frac{\beta}{t_0} \left(\frac{\sigma_{h,max} - \sigma_{h,min}}{\sigma_c} \right)^{m_2} \sigma_{h,min} > 0 \quad (5)$$

where β and m_2 are two constants normally obtained from experiments, the hydrostatic stress $\sigma_h = (\sigma_r + 2\sigma_t)/3$, σ_c is the critical stress and the subscripts min and max are the minimum and the maximum values.

(4) lithium plating model

A model where plated Li decays into dead Li over time, is proposed here to consider the three-way interaction between Lithium plating, stripping and SEI formation. The Li stripping flux N_{Li} is:

$$N_{Li} = k_{Li} \left(c_{L,exp} \left(\frac{F\alpha_{a,L}\eta_{Li}}{RT} \right) - c_e \exp \left(-\frac{F\alpha_{c,L}\eta_{LU}}{RT} \right) \right) \quad (6)$$

Where

$$\eta_{Li} = \phi_s - \phi_e - \eta_{SEI} \quad (7)$$

The transfer coefficients $\alpha_{a,Li}$ and $\alpha_{c,Li}$ were set to 0.3 and 0.7.

2.3 Simulation methods

A coupled degradation model incorporating the four primary degradation mechanisms was developed using the open-source modeling environment PyBAMM. The LG M50T cylindrical cell was selected for simulations due to the availability of a suitable parameter set for the DFN model in Chen et al. However, due to limited data, a thermal model was not included in this work, and the temperature was assumed to remain constant.

Capacity change is used as the measure of degradation. The capacity loss attributable to lithium inventory loss (encompassing SEI growth, cracking, and lithium plating) and active material loss is:

$$Q_{LLI} = \int_0^t i_s A dt = \int_0^t \frac{k_{SEI} \exp \left(\frac{-E_{SEI}}{RT} \right)}{2(1+\lambda\theta)\sqrt{t}} dt \quad (8)$$

$$Q_{AM} = \frac{Q_{L,loes}}{Q_{L,0}} = \int_0^t k_{AM} \exp \left(\frac{-E_{AM}}{RT} \right) \cdot SOC \cdot |I| dt \quad (9)$$

To demonstrate the effectiveness of the model, the CC-CV protocol outlined in Tab.1 was used to run the coupled degradation model until the battery degraded

from a fresh state (100% SOC) to a fully-aged state (60% SOC).

Tab.1 The CC-CV protocol profiles

The CC-CV protocol profiles
1. Start : check initial capacity , initial SOC =100%
2. repeat:
"Discharge at 1C until 2.5 V "
"Charge at 1 C until 4.2 V ",
"Hold at 4.2 V until C/100 "
3.Until SOC=60%
3. End: check initial capacity

The capacity loss plotted against the total charge throughput Q_{tot} is shown in Fig.3 and Fig.4, where

$$Q_{tot}(t) = \int_0^t |I(t)| dt \quad (10)$$

It is clearly showing that the majority of irreversible capacity fade is caused by SEI growth (especially SEI on cracks) during the first several cycles. As the battery ages further, capacity fade is increasingly dominated by various side reactions (red line) at the moderately-aged state, which is same as the Fig.1 mentioned. This observation also underscores the importance of developing charging strategies based on coupled aging models [7].

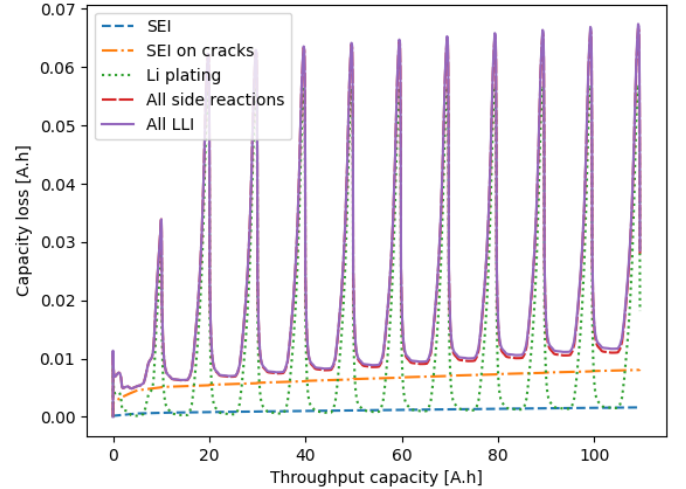


Fig.3 The capacity loss of Battery at fresh state

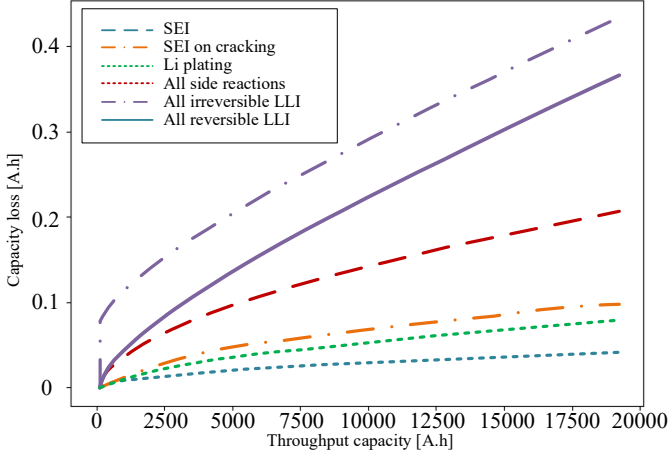


Fig.4 The capacity loss of Battery from 100%SOC to 60%SOC

3. FAST CHARGING OPTIMIZATION BASED ON RL METHOD

3.1 Design of optimized charging method

The objective of designing the ageing-aware charging profile is to suppress the coupled degradation of the cell without significantly sacrificing charging speed. As mentioned above, several key factors, including the SEI layer formation, lithium plating, active material loss and resistance growth are considered during the charging process.

The optimization problem is formulated to find the best charging current to:

$$\min_{I(t)} \gamma_1 \times (t_f - t_0) + \gamma_2 \times (SOC_{t_f} - SOC_{t_0}) + \gamma_3 \times Q_{LLI} + \gamma_4 \times Q_{AM} \quad (11)$$

Subject to:

$$I(t) = I_0 \times e^{-\frac{K}{\sqrt{C}}t} \quad (12)$$

$$\begin{aligned} I_{min} &\leq I(t) \leq I_{max} \\ V(t) &\leq V_{max} \end{aligned} \quad (13)$$

$$SOC_{t_f} = SOC_{final}, SOC_{t_0} = SOC_{init} \quad (14)$$

$$T(t_0) = T_0, V(t_0) = V_0 \quad (15)$$

$$Q_{LLI,t_0} = Q_{LLI,init}, Q_{AM,t_0} = Q_{AM,init} \quad (16)$$

Where Eq. (12) represents the charging current based on Mars theory, designed to maximize the inhibition of side effects. Here I_0 is the initial charging current, K is the current attenuation coefficient and C is the charging capacity. Eq. (13) and Eq. (14) protect against over-charging/over-discharging and high/low temperature, which accelerate

the degradation. t_0 and t_f represent the initial time and final time of charge, $t_f - t_0$, $SOC_{t_f} - SOC_{t_0}$ is the total charging time and the total charging capacity. The weighting factors γ_i are used to bring the objective terms to approximately the same order of magnitude.

It should be noted that the problem is a highly-nonlinear time-varying system with numerous constraints [9]. A deep reinforcement learning algorithm based on the deterministic policy gradient and Markov decision process (MDP) is employed to tackle this optimization problem. The MDP addresses the problem of finding the optimal policy that minimizes the total cumulative rewards from the environment. The deterministic policy gradient is a model-free deep learning algorithm that facilitates the convergence of the charging strategy training process. The state variable $X(t)$ and action variable $A(t)$ are:

$$\mathbf{X}(t) = [SOC(t) \quad V(t) \quad Q_{LLI}(t) \quad Q_{AM}(t)] \quad (17)$$

$$\mathbf{A}(t) = [I_0 \quad K \quad t] \quad (18)$$

The final algorithm proposed in this paper is summarized in Fig. 5

3.2 Reward function

The reward function plays a guiding role in using reinforcement learning algorithms for charging strategy training [5]. According to Eq.(11)-Eq.(16), the reward defined as:

$$\begin{aligned} r_{i+1} = & p_1 * r_{i+1}^{SOC} + p_2 * r_{i+1}^t + p_3 * r_{i+1}^V + p_4 * r_{i+1}^{LLI} \\ & + p_5 * r_{i+1}^{LAM} \end{aligned} \quad (19)$$

Where p_i is a tuning parameter, which provides the flexibility to emphasis the importance of different control objectives, and

$$r_{i+1}^{SOC} = 10 \times (SOC_{i+1} - SOC_i) \quad (20)$$

$$r_{i+1}^t = -0.1 \times (t_{i+1} - t_i) \quad (21)$$

$$r_{i+1}^V = \begin{cases} -(V_{i+1} - V_{max}), & V_{i+1} > V_{max} \\ 0, & V_{i+1} \leq V_{max} \end{cases} \quad (22)$$

$$r_{i+1}^{LLI} = -10^2 \times (Q_{LLI,i+1} - Q_{LLI,i}) \quad (23)$$

$$r_{i+1}^{LAM} = -10^2 \times (Q_{LAM,i+1} - Q_{LAM,i}) \quad (24)$$

In our case, the reward function is designed to encourage the battery to be charged from 20% SOC to the max SOC at the current aging stage, while minimizing the coupled degradation and keeping the voltage within the operational constraints. The upper limits of voltage $V_{max} = 4.2V$, and the charging currents are set within the range $[0.5C, 2.3C]$.

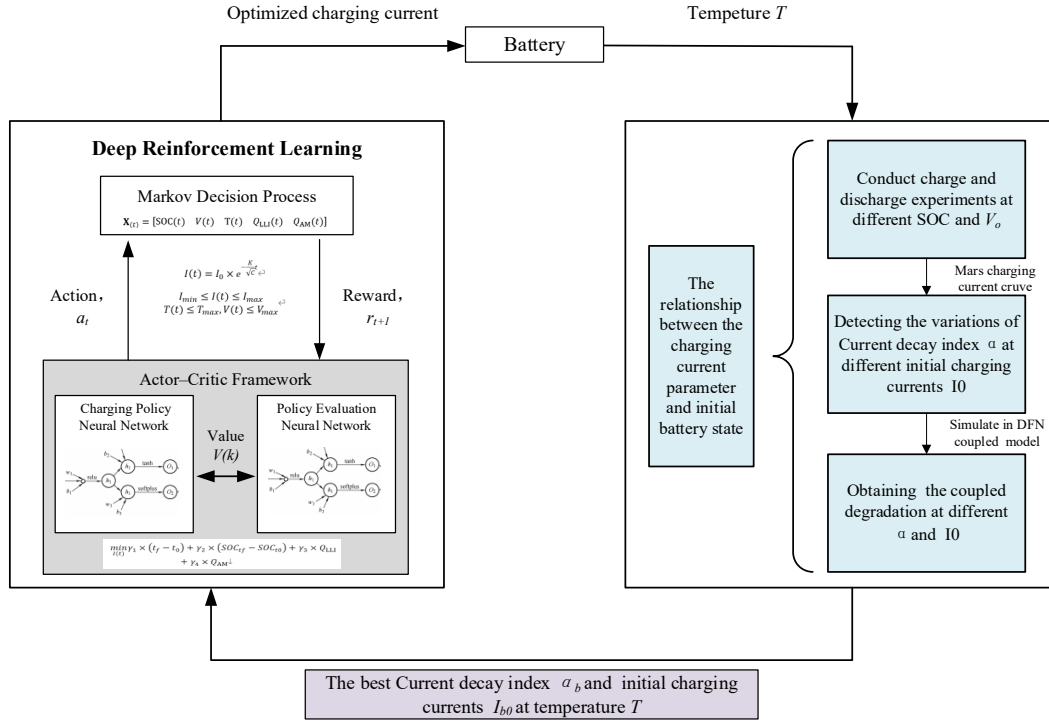


Fig.5 Flowchart of the proposed battery charging method

3.3 Charging strategy training and execution

As mentioned in Eq. (17) and Eq. (18), the state of environment is represented as a 4-D state vector comprising four entries: SOC, voltage, LLI and LAM in negative node. The action is described as a scalar of the Mars charging current with 3 parameters: I_0 , K , and charging time t . In the DDPG algorithm, The actor network is a multilayer perceptron (MLP) with two hidden layers. Each containing 40 nodes. The activation function used is the rectified linear unit (ReLU). The input to the actor network is the 4-D state vector, and the output is the action generated by the actor to be applied to the environment. The critic network is also an MLP with two hidden layers, consisting of 60 nodes in the first layer and 100 nodes in the second layer, with ReLU as the activation function. The input to the critic network is the concatenation of the state vector and the action scalar.

4. RESULTS AND DISCUSSION

The goal of this section is to verify the effectiveness of the proposed charging strategies under different degradation states. In this session, the proposed aging-aware optimal charging strategy is evaluated under different degradation stages, which are defined as follows: 1) fresh stage (100% SOC), 2) moderately aged stage (90% SOC), and 3) fully aged stage (80% SOC).

The charging speed of the battery determined by the current attenuation coefficient K , which is related to the initial charging current I_0 , the Initial SOC and the aging stages. The larger the current attenuation coefficient, the faster the charging speed. In our case. The Mars charging current curve is employed to find the initial value for optimizing charging current, thereby accelerating the convergence speed of deep learning algorithms.

The relationship between charging current parameter K , I_0 and Initial SOC is shown in Fig.6. It is clearly showing that there is a "best combination" of I_0 and Initial SOC which bring the maximum K_{max} and When Initial SOC is high, achieving a larger K requires lowering the I_0 . At the same time, As the degree of aging increases, the charging speed of the battery will progressively slow down.

To show the adaptability to variations in battery characteristics at different aging stages. The K_{max} of the optimize charging current strategy under there degradation status is shown in Fig.6, clearly shows that the optimal charging strategies are strongly affected by the battery aging status. Overall, aged battery requires the charging strategy to be more carefully regulated/controlled to avoid the degradation.

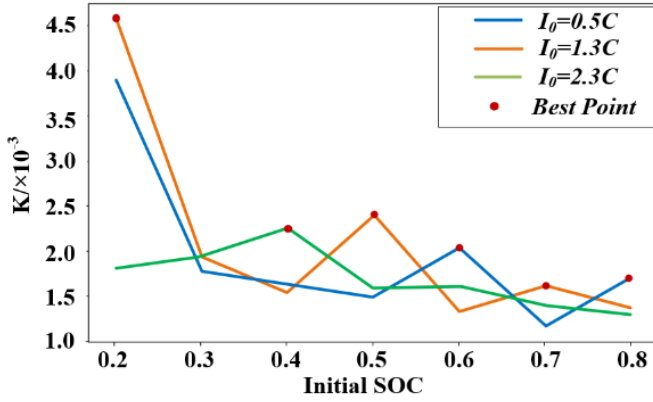


Fig. 6 The relationship between K , I_0 and Initial SOC at fresh stage

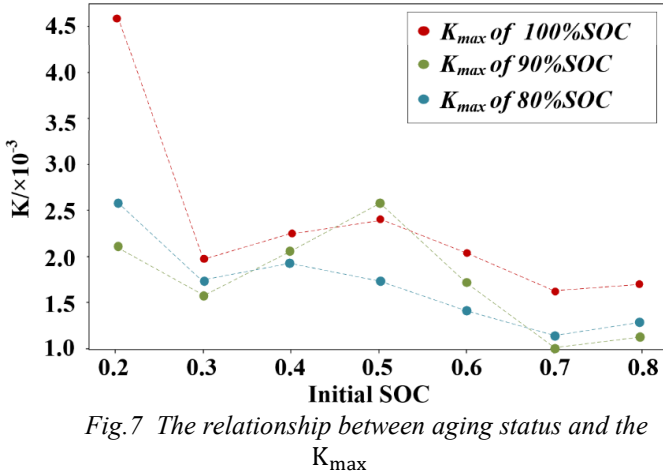


Fig. 7 The relationship between aging status and the K_{max}

5. CONCLUSIONS

This article proposed an adaptive aging-aware fast charging method utilizing deep reinforcement learning to balance charging speed with the aging effects of multiple degradation mechanisms. This method incorporates a coupled degradation model which considered four degradation mechanisms: SEI layer growth, particle cracking, active material loss, and lithium plating to capture the dynamic characteristics of batteries throughout their lifecycle. Based on the Mars charging theory, the relationships between the current attenuation coefficient K , the initial charging current I_0 and the Initial SOC are analyzed to provide initial values for the optimization charging strategy based on deep learning algorithms, thereby accelerating the convergence speed of the algorithm. The impact of battery aging status on the proposed optimal charging strategy is carefully examined. Simulations Results indicate significant adaptability to variations in battery characteristics at different aging stages.

ACKNOWLEDGEMENT

The authors declare that they have no known competing financial interests or personal relationships

that could have appeared to influence the work reported in this paper.

The authors are grateful to Dr Chongming Wang from Zephyr Intelligent System (Shanghai) Co., Ltd, Dr Dawei Qiu and Dr Yi Wang from Imperial College London, and Prof Yue Cao from Wuhan University for their insightful discussions about the energy storage systems.

REFERENCE

- [1] Han, X., Lu, L., Zheng, Y., Feng, X., Li, Z., Li, J., & Ouyang, M. (2019). A review on the key issues of the lithium ion battery degradation among the whole life cycle. *eTransportation* (Amsterdam), 1, 100005.
- [2] Bose, B., Teja, S. S., Garg, A., Gao, L., Li, W., Singh, S., & Babu, B. C. (2024). Health - Aware Battery - Fast - Charging Strategy Using Thermal - Aging Cell Model and Whale Optimization Algorithm. *Energy Technology* (Weinheim, Germany), 12(1), n/a.
- [3] Liu, C., Gao, Y., & Liu, L. (2021). Toward safe and rapid battery charging: Design optimal fast charging strategies thorough a physics - based model considering lithium plating. *International Journal of Energy Research*, 45(2), 2303–2320.
- [4] Zhou, Boru, Guodong Fan, Yansong Wang, Yisheng Liu, Shun Chen, Ziqiang Sun, Chengwen Meng, Jufeng Yang, and Xi Zhang. "Life-Extending Optimal Charging for Lithium-Ion Batteries Based on a Multi-Physics Model and Model Predictive Control." *Applied energy* 361 (2024): Applied energy, 2024-05, Vol.361, Article 122918.
- [5] Jin, Xing. "Aging-Aware Optimal Charging Strategy for Lithium-Ion Batteries: Considering Aging Status and Electro-Thermal-Aging Dynamics." *Electrochimica acta* 407 (2022): 139651.
- [6] Wu, Yue, Zhiwu Huang, Dongjun Li, Heng Li, Jun Peng, Daniel Stroe, and Ziyong Song. "Optimal Battery Thermal Management for Electric Vehicles with Battery Degradation Minimization." *Applied energy* 353 (2024): 122090.
- [7] Hao, Yuhan, Qiugang Lu, Xizhe Wang, and Benben Jiang. "Adaptive Model-Based Reinforcement Learning for Fast Charging Optimization of Lithium-Ion Batteries." *IEEE transactions on industrial informatics* 20, no. 1 (2024): 1–10.
- [8] O'Kane, Simon E. J., Weilong Ai, Ganesh Madabattula, Diego Alonso-Alvarez, Robert Timms, Valentin Sulzer, Jacqueline Sophie Edge, Billy Wu, Gregory J Offer, and Monica Marinescu. "Lithium-Ion Battery Degradation: How to Model It." *Physical chemistry chemical physics* : PCCP 24, no. 13 (2022): 799–7922.

[9] Li, Xiaoyu, Le Chen, Wen Hua, Xiaoguang Yang, Yong Tian, Jindong Tian, and Rui Xiong. "Optimal Charging for Lithium-Ion Batteries to Avoid Lithium Plating Based on Ultrasound-Assisted Diagnosis and Model Predictive Control." *Applied energy* 367 (2024): Applied energy, 2024-08, Vol.367, Article 123396.

[10] Li, Yunjian, Kuining Li, Yi Xie, Bin Liu, Jiangyan Liu, Jintao Zheng, and Wei Li. "Optimization of Charging Strategy for Lithium-Ion Battery Packs Based on Complete Battery Pack Model." *Journal of energy storage* 37 (2021): 102466.